

# Giant Intrinsic Spin and Orbital Hall Effects in $\text{Sr}_2\text{MO}_4$ ( $M=\text{Ru,Rh,Mo}$ )

H. KONTANI<sup>1</sup>, T. TANAKA<sup>1</sup>, D.S. HIRASHIMA<sup>1</sup>, K. YAMADA<sup>2</sup> and J. INOUE<sup>3</sup>

(Dated: September 5, 2018)

We investigate the intrinsic spin Hall conductivity (SHC) and the  $d$ -orbital Hall conductivity (OHC) in metallic  $d$ -electron systems, by focusing on the  $t_{2g}$ -orbital tight-binding model for  $\text{Sr}_2\text{MO}_4$  ( $M=\text{Ru,Rh,Mo}$ ). The conductivities obtained are one or two orders of magnitude larger than predicted values for  $p$ -type semiconductors with  $\sim 5\%$  hole doping. The origin of these giant Hall effects is the “effective Aharonov-Bohm phase” that is induced by the  $d$ -atomic angular momentum in connection with the spin-orbit interaction and the inter-orbital hopping integrals. The huge SHC and OHC generated by this mechanism are expected to be ubiquitous in multiorbital transition metal complexes, which opens the possibility of realizing spintronics as well as “orbitronics” devices.

PACS numbers: 72.25.Ba, 74.70.Pq, 85.75.-d

Recently, the spin Hall effect (SHE) has been attracting considerable interest since controlling spin by applying electric field is one of the key issues in the field of spintronics [1]. The SHE was originally predicted based on the assumption of extrinsic electron-scattering [2, 3]. Intrinsic SHE in semiconductors is caused by uniform spin-orbit interaction (SOI) in systems and is independent of the presence of impurities. Its existence was predicted by Murakami *et al.* [4] for  $p$ -type semiconductors, and by Sinova *et al.* [5] for a two-dimensional electron gas (2DEG) with a Rashba-type SOI. Motivated by these predictions, many studies have been performed to demonstrate the prominent disorder effects on the spin Hall conductivity (SHC) [6–9], the possibility of quantum SHE in insulating phase of semiconductors [10–12], and the existence of the orbital Hall effect (OHE). According to the result of the *ab initio* calculation [13], SHC and orbital Hall conductivity (OHC) for  $p$ -type semiconductors increase with hole number  $n_h$ , and they reach about 100 and 10 [ $\hbar e^{-1} \cdot \Omega^{-1} \text{cm}^{-1}$ ] respectively, for  $n_h = 0.05/\text{cell}$ .

Very recently, the so-called inverse SHE has been observed for spin currents injected into conventional metals such as Al and Pt from a ferromagnet [14, 15]. The SHC observed in Pt is  $\sim 240$  [ $\hbar e^{-1} \cdot \Omega^{-1} \text{cm}^{-1}$ ], which is about  $10^4$  times larger than the experimental SHC in  $n$ -type semiconductors reported in ref. [16]. This observation raises the question of whether a novel mechanism may be responsible for the *giant SHE* in  $d$ -electron systems. Moreover, a simple theoretical model that is capable of describing the giant SHE inherent in  $d$ -electron systems is highly desirable.

In this Letter, we propose a new mechanism for the giant intrinsic SHC and OHC that originate from the  $d$ -orbital degrees of freedom, which is absent in semiconductors. In a multiorbital system, a conduction electron acquires an “effective Aharonov-Bohm phase factor” due to  $d$ -atomic angular momentum in conjunction with the SOI and the inter-orbital hoppings. This mechanism is responsible for the large SHE. An intuitive explanation based on the tight-binding model, which is given in Fig. 3, appears to successfully predict the characteristics of

SHE in  $d$ -electron systems. We stress that not only the SOI play a significant role in the SHE, but so does the phase of hopping integrals characteristic of  $d$ -electron systems. In contrast, the “Dirac monopole mechanism” [4] is appropriate when massless Dirac cone dispersion exists in close proximity to the Fermi level, as is the case in semiconductors. The present mechanism of SHE also differs from that in the Rashba-type 2DEG model due to the momentum-dependent SOI [5]. We further show that the calculated SHC depends strongly on the longitudinal resistivity in the high-resistivity region, even though the SHE is of intrinsic origin.

To demonstrate the mechanism of the intrinsic SHC and OHC due to  $d$ -orbital degrees of freedom, we adopt the square-lattice tight-binding model with  $(d_{xz}, d_{yz}, d_{xy})$ -orbitals, which was first proposed to describe the realistic electron-structure of  $\text{Sr}_2\text{MO}_4$  ( $M=\text{Ru,Rh,Mo}$ ) [17], and atomic LS coupling as the SOI. This model is subsequently referred to as the  $t_{2g}$ -model. We show that the calculated SHC and OHC are one or two orders of magnitude greater than theoretical values in highly doped  $p$ -type semiconductors [13]. The present study strongly predicts that giant SHE and OHE are ubiquitous in  $d$ -electron systems, and suggests a new method to analyze them in various metals.

The Hamiltonian for the  $t_{2g}$ -model in a square lattice is given by  $H = H_K + H_{\text{SO}}$ , where  $H_K$  is the kinetic term and  $H_{\text{SO}} = \sum_i 2\lambda_i \cdot \mathbf{s}_i$  is the SOI for  $M$   $4d$ -orbitals. The band parameters of the  $t_{2g}$ -model are: (i) the intraorbital nearest neighbor (NN) hopping integrals  $t_1 = t_2 (\equiv t)$  and  $t_3$  for the  $xz, yz$  and  $xy$  orbitals, respectively, (ii) intraorbital second NN hopping  $t'_3$  for  $xy$  orbital, and (iii) interorbital second NN hopping  $t'$  between the  $xz$  and  $yz$  orbitals. It will be shown later that interorbital hopping  $t'$  is indispensable for SHE and OHE.

The matrix elements of  $H_K$  are then easily given by

$$\hat{H}_K = \begin{pmatrix} \xi_1 & g & 0 \\ g & \xi_2 & 0 \\ 0 & 0 & \xi_3 \end{pmatrix}, \quad (1)$$

where  $\xi_1 = -2t \cos k_x$ ,  $\xi_2 = -2t \cos k_y$ ,  $\xi_3 =$

$-2t_3(\cos k_x + \cos k_y) - 4t'_3 \cos k_x \cos k_y + \xi_3^0$ , and  $g = -4t' \sin k_x \sin k_y$ . Here, the first, second, and third rows (columns) of  $\hat{H}_K$  correspond to  $|xz\rangle$ ,  $|yz\rangle$ , and  $|xy\rangle$ , respectively, and 1, 2, and 3 denote orbitals  $xz$ ,  $yz$ , and  $xy$ , respectively. We set  $\hbar = 1$  during the calculation. A constant  $\xi_3^0$  is included in  $\xi_3$  to allow the number of electrons  $n_l$  in the  $l$ -orbital to be adjusted.

The total Hamiltonian is given by

$$\hat{H} = \begin{pmatrix} \hat{H}_K + \lambda \hat{l}_z & \lambda(\hat{l}_x - i\hat{l}_y) \\ \lambda(\hat{l}_x + i\hat{l}_y) & \hat{H}_K - \lambda \hat{l}_z \end{pmatrix}, \quad (2)$$

where the first and the second rows (columns) correspond to  $|\uparrow\rangle$  and  $|\downarrow\rangle$ , respectively. The matrix element of  $\hat{l}_\zeta$  ( $\zeta = x, y, z$ ) is specified in quantum mechanics textbooks as, for example,  $(\hat{l}_z)_{l,m} = i(\delta_{l,2}\delta_{m,1} - \delta_{l,1}\delta_{m,2})$ . In accordance with Refs. [17–19], we set  $t = 1$  ( $\approx 0.2$  eV),  $t' = 0.1$ ,  $t_3 = 0.8$ ,  $t'_3 = 0.35$ , and  $\lambda \sim 0.2$ . The band structure for  $\text{Sr}_2\text{RuO}_4$  is reproduced by selecting the chemical potential  $\mu$  and  $\xi_3^0$  so that  $n_1 = n_2 = n_3 = n/3$ . The Fermi surfaces for  $\lambda = 0.2$  are shown in the inset of Fig. 1. ( $\alpha, \beta$ )-bands [ $\gamma$ -band] are mainly composed of ( $d_{xz}, d_{yz}$ )-orbitals [ $d_{xy}$ -orbital] and, due to the symmetry of  $\hat{H}$  under  $\mathbf{k} \leftrightarrow -\mathbf{k}$ , each band is two-fold degenerate even if  $\lambda > 0$ , in contrast to the Rashba 2DEG model. The shape of the Fermi surfaces agrees with that obtained in the ARPES measurements, LDA band calculations, and dHvA oscillations [20].

The  $6 \times 6$  matrix retarded Green function is given by  $\hat{G}^R(\mathbf{k}, \omega) = (\omega + \mu - \hat{H} + i\hat{\Gamma})^{-1}$ , where  $\hat{\Gamma}$  is the imaginary part of the  $\mathbf{k}$ -independent self-energy due to local impurities. Since a tiny residual resistivity in  $\text{Sr}_2\text{RuO}_4$  suggests that the impurity potentials are small, we apply the Born approximation:  $\hat{\Gamma} \propto -\text{Im} \sum_{\mathbf{k}} \hat{G}^R(\mathbf{k}, 0)$ . If  $\lambda = 0$ , then  $\hat{\Gamma}$  is diagonal;  $\hat{\Gamma}_{l,m} \propto \gamma_l \delta_{l,m}$  ( $l, m = 1, 2, 3$ ). The off-diagonal terms will then be negligible if  $\lambda \ll W_{\text{band}}$ .  $\gamma_l$  is the quasiparticle damping rate for the  $l$ -orbital, and is proportional to the local density of states (LDOS) for the  $l$ -orbital,  $\rho_l(0)$ . In  $\text{Sr}_2\text{RuO}_4$ ,  $1 \ll \rho_3(0)/\rho_1(0) \sim 2.5$  since the  $\gamma$ -band Fermi surface is very close to the van-Hove singular point at  $(\pi, 0)$  [17].

The charge current for  $\zeta$ -direction ( $\zeta = x, y$ ) is given by  $\hat{J}_\zeta^C = -e \cdot d\hat{H}/dk_\zeta$  ( $-e$  is the electron charge), and the  $\sigma_z$ -spin current is given by the Hermitian operator:  $\hat{J}_\zeta^S = (-1/e)\{\hat{J}_\zeta^C, \hat{s}_z\}/2$  [4–13]. Since the SOI is  $\mathbf{k}$ -independent, they are given by

$$\hat{J}_\zeta^C = -e \begin{pmatrix} \hat{v}_\zeta & 0 \\ 0 & \hat{v}_\zeta \end{pmatrix}, \quad \hat{J}_\zeta^S = \frac{1}{2} \begin{pmatrix} \hat{v}_\zeta & 0 \\ 0 & -\hat{v}_\zeta \end{pmatrix}, \quad (3)$$

where  $\hat{v}_\zeta = d\hat{H}_K/dk_\zeta$ . Also, the  $l_z$ -orbital current is given by  $\hat{J}_\zeta^O = \{\hat{J}_\zeta^C, \hat{l}_z\}/2$  [13].

We now calculate the SHC and OHC in the presence of local impurities using the linear-response theory. In the current model,  $\hat{v}_\zeta$  and  $G$  are respectively odd and even functions with respect to  $\mathbf{k} \leftrightarrow -\mathbf{k}$ . Therefore,

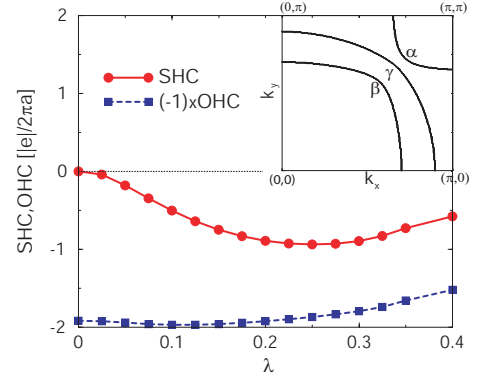


FIG. 1:  $\lambda$ -dependence of the SHC and OHC in  $\text{Sr}_2\text{RuO}_4$ . A typical value of  $\lambda$  for  $\text{Ru}^{4+}$ -ion is  $\sim 0.2$ . We set  $\gamma_1 = \gamma_2 = 0.005$  and  $\gamma_3/\gamma_1 = 3$ . Inset: Fermi surfaces of  $\text{Sr}_2\text{RuO}_4$  for  $\lambda = 0.2$ .

the current vertex correction (CVC) due to the local impurity potentials in the (extended) Born approximation, which is given by  $\Delta \hat{J}_\zeta^M \propto \sum_{\mathbf{k}} \hat{G}^A \hat{J}_\zeta^M \hat{G}^R$  ( $M=S, C$  or  $O$ ), vanishes identically. (In contrast, the CVC is crucial in the Rashba 2DEG model since the SOI, which is an odd-function with respect to  $\mathbf{k}$ , gives a  $\mathbf{k}$ -independent anomalous velocity [6].) For this reason, the SHC at  $T = 0$  is given by  $\sigma_{xy}^z = \sigma_{xy}^{zI} + \sigma_{xy}^{zII}$  [21], where

$$\sigma_{xy}^{zI} = \frac{1}{2\pi N} \sum_{\mathbf{k}} \text{Tr} \left[ \hat{J}_x^S \hat{G}^R \hat{J}_y^C \hat{G}^A \right]_{\omega=0}, \quad (4)$$

$$\sigma_{xy}^{zII} = \frac{-1}{4\pi N} \sum_{\mathbf{k}} \int_{-\infty}^0 d\omega \text{Tr} \left[ \hat{J}_x^S \frac{\hat{G}^R}{\partial \omega} \hat{J}_y^C \hat{G}^R - \hat{J}_x^S \hat{G}^R \hat{J}_y^C \frac{\hat{G}^R}{\partial \omega} - \langle R \rightarrow A \rangle \right]. \quad (5)$$

Here,  $I$  and  $II$  represent the “Fermi surface term” and the “Fermi sea term”. Taking the trace in eq. (4),  $\sigma_{xy}^{zI}$  in the present model is straightforwardly given by  $\sigma_{xy}^{zI(1)} + \sigma_{xy}^{zI(2)} + \sigma_{xy}^{zI(3)}$ , where

$$\sigma_{xy}^{zI(1)} = \frac{2e\lambda}{\pi N} \sum_{\mathbf{k}} \gamma_1 v_x^a v_y ((\mu - \xi_3)^2 + \gamma_3^2) / |D^R|^2, \quad (6)$$

$$\sigma_{xy}^{zI(2)} = \frac{e\lambda^2}{\pi N} \sum_{\mathbf{k}} [2\gamma_1 v_x^a v_y (\mu - \xi_3) + \gamma_3 (g v_x v_y + 2v_x^a v_y (\mu - \xi_3))] / |D^R|^2, \quad (7)$$

$$\sigma_{xy}^{zI(3)} = \frac{2e\lambda^3}{\pi N} \sum_{\mathbf{k}} \gamma_3 v_x^a v_y / |D^R|^2, \quad (8)$$

where  $v_\zeta^a = dg/dk_\zeta$  ( $\zeta = x, y$ ),  $v_x = d\xi_1/dk_x$ ,  $v_y = d\xi_2/dk_y$ , and  $D^R = \det(\mu - \hat{H}^s + i\hat{\Gamma})$ .  $\sigma_{xy}^{zI(m)}$  ( $m = 1, 2, 3$ ) is proportional to  $\lambda^m$  except for the  $\lambda$ -dependence of  $D^R$ . The “Fermi sea term” can also be obtained by inserting  $\hat{J}_x^{C,S}$  in eq. (3) into eq. (5). We do not give an expression

for it since its contribution is very small in the metallic state [23] (see Fig. 2 (b)).

In the same way, the OHC of the Fermi surface term  $O_{xy}^{zI}$  and that of the Fermi sea term  $O_{xy}^{zII}$  are respectively given by eqs. (4) and (5) by replacing  $\hat{J}_x^S$  with  $\hat{J}_x^O$ . In the present model,  $O_{xy}^{zI}$  is given by  $O_{xy}^{zI(0)} + O_{xy}^{zI(2)}$ , where

$$O_{xy}^{zI(0)} = \frac{e}{\pi N} \sum_{\mathbf{k}} \gamma_1 v_x [g v_y + v_y^a (\xi_1 - \xi_2)] \times ((\mu - \xi_3)^2 + \gamma_3^2) / |D^R|^2, \quad (9)$$

$$O_{xy}^{zI(2)} = \frac{e \lambda^2}{\pi N} \sum_{\mathbf{k}} \gamma_3 v_x [g v_y + v_y^a (\xi_1 - \xi_2)] / |D^R|^2. \quad (10)$$

The interorbital velocity  $v_\zeta^a = dg/dk_\zeta$  is termed the ‘‘anomalous velocity’’, which is the origin of the Hall effect [23]. Since  $v_x^a = -4t' \sin k_y \cos k_x$  has the same symmetry as  $k_y$ , eqs. (6)-(8) are finite even after the  $\mathbf{k}$ -summations. Since  $t'$  is much larger than the Rashba SOI in semiconductors, a large SHC is realized in the present model. Although the sign of  $t'$  changes due to the gauge transformation  $|xz\rangle \rightarrow -|xz\rangle$ , both the SHC and OHC are invariant if the sign change of  $(\hat{l}_\zeta)_{l,1}$  is taken into account [23]. We stress that eqs. (6)-(10) are independent of the renormalization factor due to the Coulomb interaction:  $z = (1 - \partial \Sigma(\omega) / \partial \omega)^{-1} |_{\omega=0}$  [23].

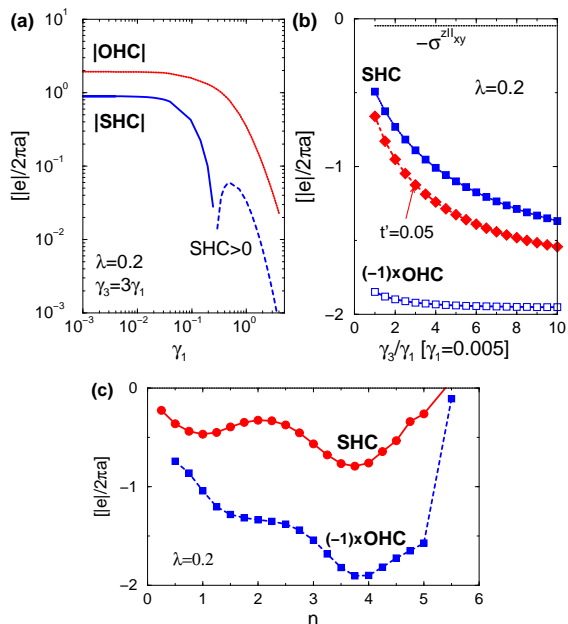


FIG. 2: (a)  $\gamma_1$ -dependence and (b)  $\gamma_3/\gamma_1$ -dependence of the |SHC| and |OHC| in  $\text{Sr}_2\text{RuO}_4$ .  $|\sigma_{xy}^z(t' = 0.05)|$  is larger than  $|\sigma_{xy}^z(t' = 0.1)|$ , which is understood from the relation  $|\sigma_{xy}^z| \propto t' \Delta^{-2}$  in the present model. (c)  $n$ -dependence of the SHC and OHC in the  $t_{2g}$ -model [ $\text{Sr}_2\text{MO}_4$ ].

Figure 1 shows the  $\lambda$ -dependence of the SHC and OHC for the  $t_{2g}$ -model with  $M=\text{Ru}$  ( $n = 4$ ). Here, we put

$\gamma_1 = \gamma_2 = 0.005$  and  $\gamma_3/\gamma_1 = 3$ . The Fermi sea terms ( $II$ ) of both the SHC and OHC are negligible [23] since they are about 30 times smaller than the Fermi surface terms ( $I$ ) given in eqs. (6)-(10) (see Fig. 2 (b)). Here,  $1.0 [e/2\pi a]$  corresponds to  $\approx 670 [\hbar e^{-1} \cdot \Omega^{-1} \text{cm}^{-1}]$  if we put the interlayer distance of  $\text{Sr}_2\text{MO}_4$ ,  $a \approx 6\text{\AA}$ . The obtained SHC and OHC for typical values of  $\lambda \sim 0.2$  are much larger than those in semiconductors [4, 13]. In Fig. 1, the SHC increases approximately in proportion to  $\lambda^2$  since  $\sigma_{xy}^{zI(2)}$  in eq. (7) gives the dominant contribution for  $0.05 < \lambda < 0.3$ . On the other hand, the OHC exists even if  $\lambda = 0$  since the orbital current is independent of spin. Note that the OHC vanishes if  $\lambda = 0$  in Rashba 2DEG model since the anomalous velocity arises from the  $\mathbf{k}$ -dependent SOI.

Figure 2 (a) shows the  $\gamma_1$ -dependences of the SHC and OHC for  $\gamma_3/\gamma_1 = 3$ . They are approximately independent of  $\gamma_1$  in the low-resistivity region where  $\gamma_1 < 0.1$ . This behavior is typical of the intrinsic Hall effect found by Karplus and Luttinger [22]. However, both the SHC and OHC start to decrease with  $\gamma_1$  in the high-resistivity region where  $\gamma_1 > 0.1$ . This crossover behavior is also realized in the intrinsic anomalous Hall effect (AHE) [23, 24]: Since the intrinsic Hall effect originates from the interband particle-hole excitation induced by the electric field [22], the Hall conductivity is proportional to the lifetime of the excitation  $\hbar/\Delta$ , where  $\Delta$  is the minimum band-splitting around the Fermi level [23]. In this model,  $\Delta \sim 0.2$ . In the high-resistivity region, the SHC decreases drastically since the interband excitation is suppressed when the quasiparticle lifetime  $\hbar/\gamma$  is shorter than  $\hbar/\Delta$ . Interestingly, the SHC becomes positive for  $\gamma_1 \geq 0.3$  since  $\sigma_{xy}^{zI(1)} (> 0)$  is dominant over  $\sigma_{xy}^{zI(2)}$ .

Even in the low-resistivity region, the SHC and OHC sensitively depend on the value of  $\gamma_3/\gamma_1$  as shown in Fig. 2 (b).  $|\sigma_{xy}^z|$  increases significantly with  $\gamma_3/\gamma_1$  since the numerator of the second term in eq. (7) and that in eq. (8) are proportional to  $\gamma_3$ . On the other hand,  $O_{xy}^z$  is approximately independent of  $\gamma_3/\gamma_1$ . Here, we consider how to increase  $\gamma_3/\gamma_1$  in real systems. According to ref. [25],  $\gamma$ -band Fermi surface touches  $(\pi, 0)$  in La-doped  $\text{Sr}_{2-y}\text{La}_y\text{RuO}_4$  for  $y \sim 0.23$  ( $n \sim 4.23$ ). Then,  $\gamma_3/\gamma_1 \gg 1$  is expected within the Born approximation. We also consider Ca-doped  $\text{Ca}_{2-y}\text{Sr}_y\text{RuO}_4$  ( $n = 4$ ): According to optical measurements [26], a huge mass-enhancement is realized in  $\gamma$ -band, whereas  $\alpha, \beta$ -bands remain light. In this situation,  $\gamma_3/\gamma_1 \gg 1$  due to inelastic scattering is expected at finite temperatures.

Figure 2 (c) shows the electron filling ( $n$ ) dependence of the SHC and OHC in the  $t_{2g}$ -model. For  $\text{Sr}_2\text{MO}_4$ ,  $M=\text{Ru}$ ,  $\text{Mo}$  and  $\text{Rh}$  correspond to  $n = 4, 2$  and  $5$ , respectively [27, 28]. Here, we correctly account for the  $n$ -dependence of  $\gamma_3/\gamma_1 = \rho_3(0)/\rho_1(0)$ . It is thus possible to control the values of SHC and OHC by varying the electron filling.

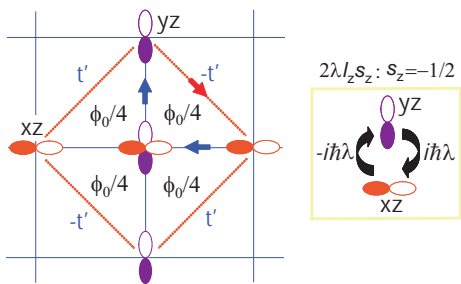


FIG. 3: “Effective magnetic flux” for  $\downarrow$ -electron through triangles of half unit cells in the  $(d_{xz}, d_{yz})$ -model. The effective magnetic flux for  $\uparrow$ -electron is  $-\phi_0/4$ .

We now present an intuitive explanation for the SHE in  $d$ -electron systems based on the  $(d_{xz}, d_{yz})$ -model [23, 31], which is a simplified version of the present model. Here, all the matrix elements of  $\hat{l}_x$  and  $\hat{l}_y$  vanish identically. In Fig. 3, we consider the motion of a  $\downarrow$ -spin electron along a triangle of a half unit cell. An electron in the  $d_{xz}$ -orbital can transfer to the  $d_{yz}$ -orbital and vice versa using the SOI for  $\downarrow$ -electron  $-\hbar\lambda\hat{l}_z$ ,  $\langle yz|\hat{l}_z|xz\rangle = -\langle xz|\hat{l}_z|yz\rangle = i$ . These relations are derived from the fact that the  $(\pi/2)$ -rotation operator about the  $z$ -axis is given by  $\exp(-i\pi\hat{l}_z/2) = \cos(\pi/2) - i\hat{l}_z \sin(\pi/2) = -i\hat{l}_z$  for  $\hat{l}_z^2 = 1$ . By considering the sign of the interorbital hopping integral ( $\pm t'$ ) and the matrix elements of the SOI, it can be shown that a clockwise (anti-clockwise) motion along any triangle of the half unit cell causes the factor  $+i$  ( $-i$ ).

This factor can be interpreted as the Aharonov-Bohm phase factor  $e^{2\pi i\phi/\phi_0}$  [ $\phi_0 = hc/e$ ], where  $\phi = \oint \mathbf{A} \cdot d\mathbf{r} = \phi_0/4$  represents the “effective magnetic flux” through the triangle of the half unit cell. Since the effective magnetic flux for  $\uparrow$ -electron is opposite in sign,  $\uparrow$ -electrons and  $\downarrow$ -electrons move in opposite directions. Thus, the effective magnetic flux in Fig. 3 gives rise to a SHC of order  $O(\lambda)$  [eq. (6)], which is analogous to the AHE due to spin chirality [29, 30]. (In the  $t_{2g}$ -model, the SHC of order  $O(\lambda^2)$  in eq. (7) is derived from the interorbital transition between  $(xy \uparrow)$  and  $(xz \downarrow)$  [or  $(yz \downarrow)$ ] using the SOI twice.) We can also discuss the origin of the OHE by considering the motion of an electron with  $|l_z = \pm 1\rangle \propto \mp|xz\rangle + i|yz\rangle$  in the absence of the SOI. Therefore, large SHE and OHE due to such an effective flux will be ubiquitous in multiorbital systems.

We comment that the  $(d_{xz}, d_{yz})$ -model has been applied to calculate the large AHE in Ru-oxides [23, 31]. Consistent with the theory, paramagnetic compound  $\text{Ca}_{1.7}\text{Sr}_{0.3}\text{RuO}_4$  exhibits large AHE under the magnetic field [32]. We find that the same mechanism, that is, the effective Aharonov-Bohm phase due to  $d$ -orbital degrees of freedom, gives rise to the large SHE and AHE.

In summary, we have studied SHC and OHC in the

$t_{2g}$ -model. The SHC obtained is about three times larger than the recently observed “giant SHC” in Pt [15], and it can be further increased by controlling  $\gamma_3/\gamma_1$ . The large SHE in our model originates from the “effective Aharonov-Bohm phase” induced by the atomic SOI and the interorbital hopping integral. Moreover, huge OHC in this model will enable us to control the atomic  $d$ -orbital state by applying an electric field. The present calculation predicts that “giant SHE and OHE” will be ubiquitous in  $d$ -electron systems. Using the theoretical technique developed here, SHC in various transition metals such as Pt had recently been investigated [33].

The authors acknowledge fruitful discussions with Y. Tanaka, S. Onari and T. Nomura. This work was supported by the Next Generation Super Computing Project, Nanoscience Program, MEXT, Japan and Grant-in-Aid for the 21st Century COE “Frontiers of Computational Science”.

- 
- [1] For an overview see e.g., *Semiconductor Spintronics and Quantum Computation*, ed. by D.D. Awschalom et al. (Springer, Berlin, 2002).
  - [2] M. I. D'yakonov et al., ZhETF Pis. Red. **13**, 657 (1971).
  - [3] J. E. Hirsch, Phys. Rev. Lett. **83**, 1834 (1999).
  - [4] S. Murakami et al., Science **301**, 1348 (2003).
  - [5] J. Sinova et al., Phys. Rev. Lett. **92**, 126603 (2004).
  - [6] J. Inoue et al., Phys. Rev. B **70**, 041303 (2004).
  - [7] S. Murakami, Phys. Rev. B **69**, 241202(R) (2004).
  - [8] B. A. Bernevig et al., Phys. Rev. Lett. **95**, 16801 (2005).
  - [9] J. Inoue et al., Phys. Rev. Lett., **97**, 46604 (2006).
  - [10] S. Murakami et al., Phys. Rev. Lett., **93**, 156804 (2004).
  - [11] C. L. Kane and E. J. Mele, Phys. Rev. Lett., **95**, 146802 (2005).
  - [12] B. A. Bernevig et al., Science **314**, 1757 (2006).
  - [13] G. Y. Guo et al., Phys. Rev. Lett. **94**, 226601 (2005).
  - [14] S. Valenzuela et al., Nature **442**, 176 (2006).
  - [15] T. Kimura et al., Phys. Rev. Lett. **98**, 156601 (2007).
  - [16] J. Wunderlich et al., Phys. Rev. Lett. **94**, 047204 (2005).
  - [17] K.K. Ng and M. Sigrist., Europhys. Lett. **49**, 473 (2000).
  - [18] T. Nomura and K. Yamada., J. Phys. Soc. Jpn. **71**, 1993 (2002); Y. Yanase and M. Ogata., J. Phys. Soc. Jpn. **72**, 673 (2003).
  - [19] T. Mizokawa et al., Phys. Rev. Lett. **87**, 077202 (2001).
  - [20] A.P. Mackenzie and Y. Maeno, Rev. Mod. Phys. **75**, 657 (2003).
  - [21] P. Streda: J. Phys. C: Solid State Phys. **15** (1982) L717.
  - [22] R. Karplus and J.M. Luttinger, Phys. Rev. **95**, 1154 (1954).
  - [23] H. Kontani et al., Phys. Rev. B **75** (2007) 184416.
  - [24] H. Kontani and K. Yamada, J. Phys. Soc. Jpn. **63**, 2627 (1994).
  - [25] N. Kikugawa et al., Phys. Rev. B **70**, 134520 (2004).
  - [26] J. S. Lee et al., Phys. Rev. Lett. **96**, 057401 (2006).
  - [27] S. Ikeda et al., J. Phys. Soc. Jpn. **69** (2000) 3162.
  - [28] F. Baumberger et al., Phys. Rev. Lett. **96**, 246402 (2006).
  - [29] M. Taillefumier et al., Phys. Rev. B **74**, 085105 (2006).
  - [30] K. Ohgushi et al., Phys. Rev. B **62**, R6065 (2000).
  - [31] M. Miyazawa et al., J. Phys. Soc. Jpn. **68** (1999) 1625.

- [32] L.M. Galvin et al., Phys. Rev. B **63**, 161102(R) (2001).
- [33] H. Kontani et al., J. Phys. Soc. Jpn. **76**, 074707 (2007);

T. Tanaka et al., arXiv: 0711.1263.